A SYNTHESIS-BASED APPROACH TO COMPRESSIVE MULTI-CONTRAST MAGNETIC RESONANCE IMAGING

Alper Güngör[1], *Emre Kopanoglu*[1], *Tolga Cukur*[2], *H. Emre Güven*[1]

ABSTRACT

In this study, we deal with the problem of image reconstruction from compressive measurements of multi-contrast magnetic resonance imaging (MRI). We propose a synthesis based approach for image reconstruction to better exploit mutual information across contrasts, while retaining individual features of each contrast image. For fast recovery, we propose an augmented Lagrangian based algorithm, using Alternating Direction Method of Multipliers (ADMM). We then compare the proposed algorithm to the state-of-the-art Compressive Sensing-MRI algorithms, and show that the proposed method results in better quality images in shorter computation time.

Index Terms— Multi-Contrast Magnetic Resonance Imaging, Compressive Sensing, ADMM

1. INTRODUCTION

Magnetic Resonance Imaging (MRI) is an imaging modality that allows high resolution imaging of soft tissues using non-ionizing radiation. In clinical usage, multiple type of scans that produce different contrast images are typically used for diagnosis. While each contrast image has different features, a significant amount of structural correlation exists between different contrast images. Furthermore, the imaging process is inherently slow due to imaging physics, making multi-contrast imaging not only costly, but also uncomfortable to the patient, and even impractical in some cases.

Compressive sensing (CS) is a signal processing approach that enables reconstruction of signals from under-sampled measurements [1, 2]. It relies on sparsity of the signal in a transformation domain, and the decrease in sparsity level improves the reconstructed image quality. Although CS has been successfully applied to MRI [1, 3, 4], exploiting correlated features in multi-contrast MRI (MC-MRI) is a relatively new research direction [3].

Alternating direction method of multipliers (ADMM) techniques have been successfully applied to signal and image recovery problems [5]. ADMM uses a divide-and-conquer approach by splitting unconstrained multi-objective convex optimization problems, augmenting the Lagrangian with a norm-squared error term, and using a nonlinear block Gauss-Seidel approach on the terms in the sub-problems. The resulting algorithm exhibits guaranteed convergence under mild conditions [5]. Various algorithms within the ADMM framework have proven useful in the context of imaging with applications in Synthetic Aperture Radar using a similar model to MRI [6]. These algorithms are especially effective where a fast transform is available for relating the unknown image to the observation vector, such as with Fast Fourier Transforms.

Here we propose a synthesis based approach to multi-contrast MRI problem. We use an ADMM based algorithm for fast image recovery of compressive multi-contrast MRI. The algorithm reconstructs each contrast image as a sum of two parts, *correlated* and *independent*, and solves for each part by minimizing a hybrid cost function using the respective objective functions. This is based on ℓ_1-synthesis based approach in the literature [2, 7]. Then, we compare our algorithm to the state-of-the-art techniques in terms of image quality, peak signal-to-noise-ratio (pSNR), and computation time.

2. OBSERVATION MODEL

Many imaging techniques assume physical models based on linear operators, in relating image vector $\mathbf{x} \in \mathbf{C}^N$ to the observation vector $\mathbf{y} \in \mathbf{C}^M$. The observation matrix $\mathbf{B}$ is then an element of $\mathbf{C}^{M \times N}$. Including the noise vector $\mathbf{n} \in \mathbf{C}^M$, the problem has the following model:

$$\mathbf{y} = \mathbf{B}\mathbf{x} + \mathbf{n}, \tag{1}$$

where $\mathbf{n}$ is typically from a normal distribution. Moreover, some imaging applications deal with a multi-channel reconstruction problem. Even though the input data from different channels or contrasts have different data vectors, joint reconstruction of these channels often increases performance [3, 8], since the underlying anatomy is the same. For channel i, the governing equation is denoted by

$$\mathbf{y}^{(i)} = \mathbf{B}^{(i)}\mathbf{x}^{(i)} + \mathbf{n}^{(i)}, \tag{2}$$

where $\mathbf{y}^{(i)}$, $\mathbf{B}^{(i)}$, $\mathbf{x}^{(i)}$, and $\mathbf{n}^{(i)}$ denote the same variables as in Eq. (1), for respective channels. In this study we tackle

[1] ASELSAN Research Center, Ankara, Turkey

[2] Electrical and Electronics Engineering Department, Ihsan Dogramaci Bilkent University, Ankara, Turkey

{alpergungor, ekopanoglu, heguven}@aselsan.com.tr, cukur@ee.bilkent.edu.tr

978-1-5090-1172-8/17/$31.00 ©2017 IEEE

the problem of joint image reconstruction from MC-MRI data. We use the joint reconstruction approach for MC-MRI by treating Proton-Density (PD), T1-weighted (T1w), T2-weighted (T2w) images as different channel data [3]. For MRI, the observation matrix $\mathbf{B}^{(i)}$ is the linear operator associated with partial Fourier observations.

3. METHOD

In this section, we first describe the proposed synthesis-based approach, then propose an efficient algorithm for the solution.

3.1. Approach

Synthesis and analysis are two common approaches to image recovery problems [7]. Compressive sensing guarantees exact reconstruction for analysis based approaches, even with redundant dictionaries [2]. Although it is previously applied in the compressive sensing framework, well-known boundaries for exact recovery are not yet established for synthesis model [2, 9, 7]. In this work, we show that synthesis based approach to multi-contrast MRI improves the quality of reconstructed images over alternative approaches.

Previous work has shown that the joint reconstruction of multi-contrast images improves image quality. In this work, we assume that each contrast image ($\mathbf{x}^{(i)}$) is sum of two components as *correlated* ($\mathbf{x}_1^{(i)}$) and *independent* ($\mathbf{x}_2^{(i)}$), such that $\mathbf{x}^{(i)} = \mathbf{x}_1^{(i)} + \mathbf{x}_2^{(i)}$. We impose joint objective functions on the *correlated* parts, and individual objectives on the *independent* parts. Let us now formulate the problem as:

$$\begin{aligned} \underset{\mathbf{x}_1,\mathbf{x}_2}{\text{minimize}} \quad & \alpha_1 f_1(\mathbf{x}_1) + \alpha_2 f_2(\mathbf{x}_1) + \beta_1 g_1(\mathbf{x}_2) + \beta_2 g_2(\mathbf{x}_2) \\ \text{subject to} \quad & \|\mathbf{B}^{(i)}(\mathbf{x}_1^{(i)} + \mathbf{x}_2^{(i)}) - \mathbf{y}^{(i)}\|_2 \le \epsilon_i,\ i \in \{1, \cdots, k\} \end{aligned} \tag{3}$$

for k contrasts, f_1, f_2 are separable objective functions for $\mathbf{x}_1$, and g_1, g_2 are separable objective functions for $\mathbf{x}_2$. Here we use f_1, f_2 as joint objective functions and g_1, g_2 as individual penalty functions while other choices are also possible.

We use the ADMM framework to solve the problem shown in (3), which is converted to the general ADMM form:

$$\begin{aligned} \underset{\mathbf{x},\mathbf{z}}{\text{minimize}} \quad & \phi_1(\mathbf{x}) + \phi_2(\mathbf{z}) \\ \text{subject to} \quad & \mathbf{G}\mathbf{x} + \mathbf{Q}\mathbf{z} - \mathbf{r} = 0, \end{aligned} \tag{4}$$

Let $\mathbf{G}_i^H = -\begin{bmatrix} (\mathbf{B}^{(i)})^H & \mathbf{I} & \mathbf{I} & 0 & 0 \\ (\mathbf{B}^{(i)})^H & 0 & 0 & \mathbf{I} & \mathbf{I} \end{bmatrix}$, $\mathbf{Q} = \mathbf{I}$, and $\mathbf{z}^{(i)} = \left[\mathbf{z}^{(i,0)^T}\mathbf{z}^{(i,1)^T}\cdots\mathbf{z}^{(i,4)^T}\right]^T$ for all $i \in \{1, \cdots, k\}$. We define $\mathbf{G}$ as a block-diagonal matrix with diagonal entries consisting of $\mathbf{G}_i$'s. This setting ensures that $\mathbf{z}^{(i,0)} = \mathbf{B}^{(i)}\left(\mathbf{x}_1^{(i)} + \mathbf{x}_2^{(i)}\right)$, $\mathbf{z}^{(i,1)} = \mathbf{x}_1^{(i)}$, $\mathbf{z}^{(i,2)} = \mathbf{x}_1^{(i)}$, $\mathbf{z}^{(i,3)} = \mathbf{x}_2^{(i)}$, and $\mathbf{z}^{(i,4)} = \mathbf{x}_2^{(i)}$.

Algorithm 1: *Multi-Contrast Synthesis-ADMM*

1. Set $n = 0$, choose $\mu > 0$, $\mathbf{z}_0^{(i,t)}$, $\mathbf{d}_0^{(i,t)}$, α_t for all $i \in \{1, \cdots, k\}$, $t \in \{0, \cdots, 4\}$.
2. **repeat**
3. **parfor** $i = 1, \cdots, k$
4. Update $\mathbf{x}_1^{(i)}$ using (9)
5. Update $\mathbf{x}_2^{(i)}$ using (10)
6. $\mathbf{z}_{n+1}^{(i,0)} = \mathbf{\Psi}_{\iota_{E\left(\epsilon,\mathbf{I},\mathbf{y}^{(i)}\right)}}\left(\mathbf{B^{(i)}}\left(\mathbf{x}_1^{(i)} + \mathbf{x}_2^{(i)}\right) - \mathbf{d}_n^{(i,0)}\right)$
7. $\mathbf{d}_{n+1}^{(i,0)} = \mathbf{d}_n^{(i,0)} - \mathbf{B^{(i)}}\left(\mathbf{x}_1^{(i)} + \mathbf{x}_2^{(i)}\right) + \mathbf{z}_{n+1}^{(0)}$
8. **endfor**
9. **parfor t = 1, 2**
10. $\left\{\mathbf{z}^{(i,t)} = \mathbf{\Psi}_{f_t \frac{\alpha_t}{\mu}}\left(\mathbf{x}_1^{(i)} - \mathbf{d}_n^{(i,t)}\right)\right\}_{i=1,\cdots,k}$
11. $\mathbf{d}_{n+1}^{(i,t)} = \mathbf{d}_n^{(i,t)} - \mathbf{x}_1^{(i)} + \mathbf{z}_{n+1}^{(i,t)}$, for all t,i
12. $\left\{\mathbf{z}^{(i,t+2)} = \mathbf{\Psi}_{g_t \frac{\beta_t}{\mu}}\left(\mathbf{x}_2^{(i)} - \mathbf{d}_n^{(i,t+2)}\right)\right\}_{i=1,\cdots,k}$
13. $\mathbf{d}_{n+1}^{(i,t+2)} = \mathbf{d}_n^{(i,t+2)} - \mathbf{x}_2^{(i)} + \mathbf{z}_{n+1}^{(i,t+2)}$, for all t,i
14. **endfor**
15. $n \leftarrow n + 1$
16. **until** some stopping criterion is satisfied.

We can then set the data fidelity constraint on $\mathbf{z}^{(i,0)}$ vectors for each contrast, and each separable constraint on the dual variable. For constraint, we use a previous approach [5] and impose the constraint using the same $\iota_{E(\epsilon_i,\mathbf{I},\mathbf{y}^{(i)})}\left(\mathbf{z^{(i,0)}}\right)$ for each contrast i.

To impose the objective functions, we set $\phi_1(\mathbf{x}) = 0$, and

$$\begin{aligned} \phi_2(\mathbf{z}) = {} & \alpha_1 f_1\left(\left\{\mathbf{z}^{(i,1)}\right\}_{i=1,\cdots,k}\right) + \alpha_2 f_2\left(\left\{\mathbf{z}^{(i,2)}\right\}_{i=1,\cdots,k}\right) \\ & + \beta_1 g_1\left(\left\{\mathbf{z}^{(i,3)}\right\}_{i=1,\cdots,k}\right) + \beta_2 g_2\left(\left\{\mathbf{z}^{(i,4)}\right\}_{i=1,\cdots,k}\right) \\ & + \sum_{i=1}^{k} \iota_{E(\epsilon_i,\mathbf{I},\mathbf{y}^{(i)})}\left(\mathbf{z^{(i,0)}}\right). \end{aligned} \tag{5}$$

3.2. Fast Solution

In this section, we describe a fast implementation of the algorithm, and present the associated update steps. Using the variable splitting procedure as given in sec. 3.1, we reach Algorithm 1. The following update equations can be used for a fast implementation of the algorithm.

$$\mathbf{r}_n^{(i,1)} = \sum_{t=1}^{2} \mathbf{z}_n^{(i,t)} + \mathbf{d}_n^{(i,t)} \tag{6}$$

Data(Ratio)	FCSA-MT	recPF	IADMM	Proposed
AB(25%)	24.87	32.52	33.08	33.57
AB(12.5%)	22.54	27.03	27.09	28.29
SR(25%)	46.04	35.54	39.69	46.84
SR(6.25%)	30.46	27.62	28.12	32.22

Table 1: Average pSNR values in dB for FCSA-MT, recPF, Individual ADMM and Proposed Method

$$\mathbf{r}_n^{(i,2)} = \sum_{t=3}^{4} \mathbf{z}_n^{(i,t)} + \mathbf{d}_n^{(i,t)} \tag{7}$$

$$\mathbf{q}_n^{(i)} = \mathbf{B}^{(i)} \left(\mathbf{r}_n^{(i,1)} + \mathbf{r}_n^{(i,2)} \right) + 2 \left(\mathbf{z}_n^{(i,0)} + \mathbf{d}_n^{(i,0)} \right) \tag{8}$$

$$\mathbf{x}_1^{(i)} = \frac{1}{2}\mathbf{r}_n^{(i,1)} - \frac{1}{8}(\mathbf{B}^{(i)})^H \mathbf{q}_n^{(i)} \tag{9}$$

$$\mathbf{x}_2^{(i)} = \frac{1}{2}\mathbf{r}_n^{(i,2)} - \frac{1}{8}(\mathbf{B}^{(i)})^H \mathbf{q}_n^{(i)} \tag{10}$$

$$\mathbf{B}^{(i)}\mathbf{x}_1^{(i)} = \frac{1}{2}\mathbf{B}^{(i)}\mathbf{r}_n^{(i,1)} - \frac{1}{8}\mathbf{q}_n^{(i)} \tag{11}$$

$$\mathbf{B}^{(i)}\mathbf{x}_2^{(i)} = \frac{1}{2}\mathbf{B}^{(i)}\mathbf{r}_n^{(i,2)} - \frac{1}{8}\mathbf{q}_n^{(i)} \tag{12}$$

Operations defined through (6) to (12) can be carried out using 3 FFTs per iteration per contrast. The $\mathbf{z}$-update step can be decomposed into sub-problems for each objective function as described in [6], and their respective proximal mapping functions can be used to carry out these steps. The resulting steps are summarized in Algorithm 1.

4. RESULTS

We set $f_1(\cdot)$ to Color Total Variation (CTV) [8], $f_2(\mathbf{v})$ to group sparsity function as $\|\mathbf{v}\|_{2,1}$, $g_1(\cdot)$ to sum of isotropic Total Variation (TV) functions for each contrast [5], and $g_2(\mathbf{v}) = \sum_i \|\mathbf{v}^i\|_1$. We use Chambolle's algorithm [5] for TV and CTV related functions and exact solutions for ℓ_1-norm based sparsity functions as proximal mappings.

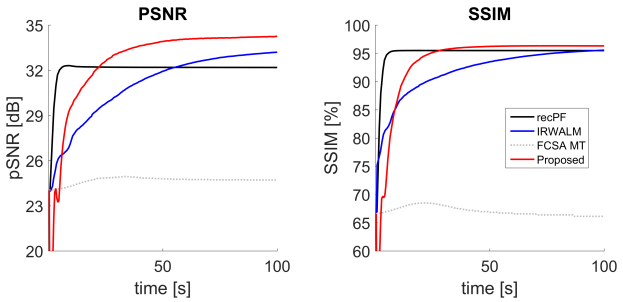

Fig. 1: pSNR and SSIM values with respect to cumulative computation time for competing methods.

We implemented Algorithm 1 in MATLAB, where group Chambolle projections ran within a mex function. We compared the algorithm with other compressive sensing MRI algorithms. The experiments were conducted on a workstation with two Intel Xeon E5-2650 v2 CPU's and 64 GB of RAM. All $\mathbf{z}_0^{(i,t)}$ values were initialized to the zero-filling reconstructions, defined as $\mathbf{z}_0^{(i,t)} = (\mathbf{B}^{(i)})^H \mathbf{y}^{(i)}$ for $t = 1, \cdots, 4$, $\mathbf{z}_0^{(i,0)} = \mathbf{y}^{(i)}$ and all Lagrangian variables $\mathbf{d}_0^{(i,t)}$ were initialized to zero vectors. All images were normalized to $[0, 255]$, and the step size parameter μ was selected as 0.01. All algorithms were run for 100 seconds.

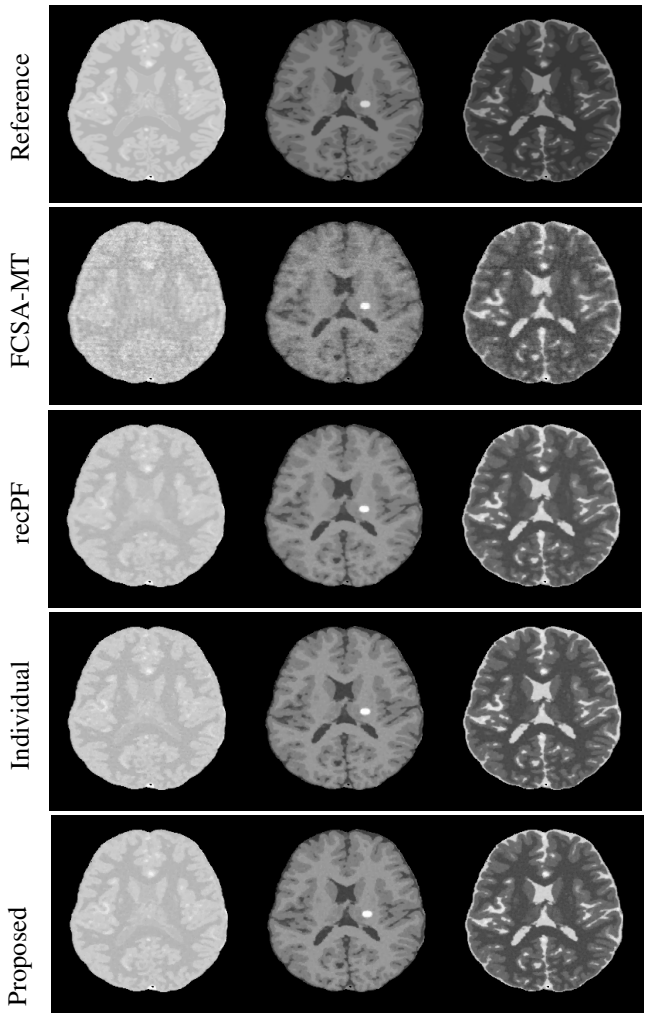

Fig. 2: The contrasts from left to right: Proton Density (PD), T1-weighted (T1w), T2-weighted (T2w) images for BP with 25% of the full data available.

First, we ran Monte Carlo simulations on FCSA-MT [3], Individual ADMM reconstructions using the algorithm in [6], recPF (reconstruction from partial Fourier observations) [4], and the proposed method, using different data subsampling patterns in each run. MATLAB codes provided by the authors of the respective methods were used for other algorithms for comparison, in which recPF was also implemented using a mex function for TV calculation. Two different complex-valued image data-sets were used; Aubert-Broche brain phantom (AB) [10], subsampled by 25% and 12.5%, and the SRI24 atlas (SR) [3], subsampled by 25%

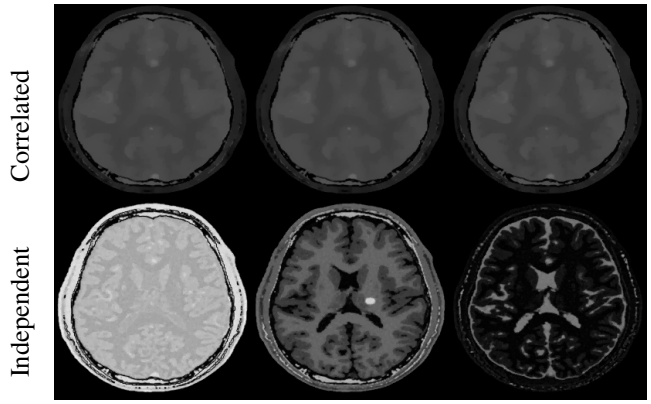

Fig. 3: Division of images as *correlated* and *independent*. Scales were adjusted to [0, 200] for all images for comparison.

and 6.25%. All three contrasts were subsampled at the same rates within each experiment, and noise was added. Parameters of all algorithms were optimized for highest structural similarity index measure (SSIM). For the proposed method, parameters were selected as: $\alpha_{JTV} = 0.0159$, $\alpha_{G\ell_1} = 1.59$, $\beta_{TV} = 0.0092$, $\beta_{\ell_1} = 0.92$. For ϵ_i, we simulated an MRI acquisition with no RF excitation to acquire noise, then, set ϵ_i to the ℓ_2-norm of the collected sample noise vector.

Figure 1 shows the reconstruction structural-similarity-index-measure (SSIM) and peak signal-to-noise ratio (pSNR) performance for all algorithms with respect to time, which was calculated using the cputime routine provided in MATLAB. The proposed method outperforms competing methods and has the fastest convergence speed with the highest pSNR. The result of Monte Carlo simulations can be found in Table I, which shows that the proposed method has higher performance on average.

Next, we analyze the reconstructed images in terms of quality. Figure 2 shows that FCSA-MT [3] results in noise-like artifacts, while recPF [4] results in an overly smoothed reconstruction. Individual method produces a relatively noisier image especially for the PD image. The proposed method has better overall quality in comparison.

Figure 3 shows the division of images as *correlated* and *independent*. Consistent with the cost functions imposed on each, similar features of contrast images were gathered in the correlated parts of the images, and individual distinctive features were gathered in independent parts.

5. CONCLUSIONS

In this study, we proposed a novel synthesis based approach to multi-contrast magnetic resonance imaging, and presented a fast solution. The method separates the image into two components, and imposes joint objective functions on one part while imposing individual objective functions on the other. We solve the resulting problem using ADMM. We also derived the necessary equations for the fast implementation of the method. We then show the effectiveness of the algorithm on two different complex and noisy sets of data in terms of both pSNR and computation time.

6. REFERENCES

[1] M. Lustig, D. Donoho, and J.M. Pauly, "Sparse mri: The application of compressed sensing for rapid mr imaging," *Magn. Reson. Med.*, vol. 58, no. 6, pp. 1182–95, Dec. 2007.

[2] E.J. Candes, Y.C. Eldar, D. Needell, and P. Randall, "Compressed sensing with coherent and redundant dictionaries," *Appl. Comput. Harmon. Anal.*, vol. 31, pp. 59–73, Jul. 2011.

[3] J. Huang, C. Chen, and L. Axel, "Fast multi-contrast mri reconstruction," *Magn. Reson. Imaging*, vol. 32, no. 10, pp. 1344–52, Sept. 2014.

[4] J. Yang, Y. Zhang, and W. Yin, "A fast alternating direction method for tvl1-l2 signal reconstruction from partial fourier data," *IEEE Journal of Selected Topics in Signal Processing*, vol. 4, pp. 288–297, Apr. 2010.

[5] M. Afonso, J. M. Bioucas-Dias, and M.A.T. Figueiredo, "An augmented lagrangian approach to the constrained optimization formulation of imaging inverse problems," *IEEE Trans. Image Processing*, vol. 20, pp. 681–95, Mar. 2011.

[6] H. E. Guven, A. Gungor, and M. Cetin, "An augmented lagrangian method for complex-valued compressed sar imaging," *IEEE Trans. Comp. Imaging*, vol. 2, no. 3, pp. 235–250, Sept. 2016.

[7] A. Majumdar and R. K. Ward, "Synthesis and analysis prior algorithms for joint-sparse recovery," in *IEEE Int. Conf. Acoust. Speech and Signal Process (ICASSP)*, Mar. 2012, pp. 3421–24.

[8] X. Bresson and T. F. Chan, "Fast dual minimization of the vectorial total variation norm and applications to color image processing," *Inverse Problems and Imaging*, vol. 2, pp. 455–84, 2008.

[9] Hui Zhang, Ming Yan, and Wotao Yin, "One condition for solution uniqueness and robustness of both l1-synthesis and l1-analysis minimizations," *Adv. Comp. Math.*, pp. 1–19, 2016.

[10] B. Aubert-Broche, M. Griffin, G. B. Pike, A. C. Evans, and D. L. Collins, "Twenty new digital brain phantoms for creation of validation image data bases," *Trans. Med. Imaging*, vol. 25, pp. 1410–16, 2006.